Influence of Collision Energy on the Nascent OH($X^2\Pi$, $v'' = 0-4$) Product Energetics for the Reaction of O(^1D) with Ethane. A Laser-Induced Fluorescence and Quasiclassical Trajectory Study

Miguel González,*,† María P. Puyuelo,‡ Jordi Hernando,† R. Sayós,† Pedro A. Enríquez,‡ and Javier Guallar‡

Departament de Química Física i Centre de Recerca en Química Teòrica, Universitat de Barcelona, C/ Martí i Franquès, 1, 08028 Barcelona, Spain, and Departamento de Química, Universidad de La Rioja, C/ Madre de Dios, 51, 26004 Logroño, Spain

Received: May 1, 2001; In Final Form: July 12, 2001

The full characterization of the nascent OH($X^2\Pi$, v'', N'', J'', Λ'') state distributions for the O(^1D) + $C_2H_6 \rightarrow$ OH + C_2H_5 reaction has been experimentally performed using the laser-induced fluorescence technique to probe the $v'' = 0-4$ levels of the OH molecules. This thorough study has been carried out for the first time using the N_2O photodissociation at 193 nm to generate the O(^1D) atoms (the average collision energy, $\langle E_T \rangle$, is equal to 0.52 eV). By comparison with the experimental available data for $\langle E_T \rangle = 0.27$ eV (Park and Wiesenfeld, *J. Chem. Phys.* **1991**, *95*, 8166), it has been observed the existence of a small influence of E_T on the dynamics of the title reaction, as only a somewhat higher rovibrational excitation of the OH product has been found on increasing the collision energy of the system. This supports the belief that the studied reaction essentially evolves through the insertion of the O(^1D) atom into a C−H bond, yielding both short-lived (insertion/fast elimination microscopic mechanism) and long-lived (insertion/slow elimination microscopic mechanism) alcohol-type collision complexes. However, although not fully conclusive, some evidence has been found about the coexistence of a third reaction mode (abstraction), which may contribute to the formation of the highest vibrationally excited OH molecules with low rotational excitation. The dynamics of the insertion/fast elimination mechanism has been qualitatively reproduced using the quasiclassical trajectory method applied on two ab initio based analytical triatomic potential energy surfaces developed by us very recently for the related O(^1D) + CH_4 reaction, but with a mass correction.

I. Introduction

The reactions of the oxygen atom in its first excited electronic state, O(^1D), with hydrocarbons are an important source for stratospheric OH molecules, which are involved in the natural degradation processes of the ozone layer through the OH/HO_2 catalytic cycle.[1−3] Though most studies of these reactions have focused on the O(^1D) + CH_4 process, an increasing number of them explore the properties of the reactions with larger hydrocarbons.

The global (including all reaction channels) rate constant (k) for the O(^1D) + C_2H_6 process falls near the gas kinetic value; it is equal to $(6.3 \pm 0.3) \times 10^{-10}$ cm^3 molecule^{-1} s^{-1} [4] at 300 K. The reaction channel leading to the formation of OH radicals,

$$O(^1D) + C_2H_6 \rightarrow OH(X^2\Pi) + C_2H_5 \qquad \Delta H^\circ_{298K} = -49.1 \text{ kcal mol}^{-1} \text{ (ref 5)} \quad (1)$$

is minor in this case, in contrast to the reaction between O(^1D) and CH_4. The observed yield for OH production in the process with CH_4 is equal to 0.75 ± 0.15,[6] while the one for reaction 1 is equal to 0.25.[7] This difference has been atributted to the preference for the cleavage of the C−C bond instead of the C−O bond in the alcoholic C_2H_5OH intermediate through which the reaction is believed to evolve. In this sense, the yield of the reaction channels not producing OH, H, or the quenching of O(^1D) atom has been estimated as 0.87 for the process between O(^1D) and C_2H_6,[4] and more recently, a value of 0.70 has been reported for the branching ratio of the $CH_3 + CH_2OH$ channel.[7]

Some experimental work can be found in the literature devoted to the determination of the nascent quantum state distributions of the OH product arising from reaction 1. Full characterization of the OH($X^2\Pi$) molecules was performed at an average collision energy of reactants ($\langle E_T \rangle$) equal to 0.27 eV, using the 248 nm photolysis of O_3 as a source of O(^1D) atoms.[8] The OH vibrational levels from $v'' = 0$ to $v'' = 4$ were detected by means of the laser-induced fluorescence (LIF) technique. A monotonically descendent vibrational distribution, a bimodal rotational distribution for $v'' = 0$ in contrast with the unimodal rotational profiles for $v'' = 1-4$, a statistical OH($X^2\Pi_{3/2}$)/OH($X^2\Pi_{1/2}$) spin−orbit population ratio, and a quite slight preference for the population of the OH($X^2\Pi$, $\Pi(A')$) Λ-doublet state were observed.[8] These results are in agreement with a previous study of the OH($X^2\Pi$, $v'' = 0-1$) distributions at a similar collision energy.[9] The OH($X^2\Pi$, $v'' = 0, 1$) product state distributions arising from reaction 1 have also been measured at a higher collision energy, $\langle E_T \rangle = 0.52$ eV, using the 193 nm photolysis of N_2O as a source of O(^1D) atoms.[10−12] This is a cleaner source of O(^1D) atoms than the photolysis of O_3 at 248 nm. Results similar to those determined at $\langle E_T \rangle = 0.27$ eV were obtained at $\langle E_T \rangle = 0.52$ eV, although somewhat

* To whom correspondence should be addressed. E-mail: miguel@qf.ub.es. Fax: +34-93-4021231.
† Universitat de Barcelona.
‡ Universidad de La Rioja.

10.1021/jp011634a CCC: $20.00
Published on Web 10/05/2001

more rotational excitation of the OH product was found. Nevertheless, to achieve a better understanding of the effect of collision energy on the dynamical properties of the $OH(X^2\Pi)$ product, the characterization of its nascent quantum state distributions for the full range of populated vibrational levels at the $\langle E_T \rangle = 0.52$ eV condition would be very useful.

The stereodynamics of reaction 1 has been examined using polarized Doppler resolved LIF spectroscopy.[13] Differential cross sections ($\mathbf{k} - \mathbf{k}'$) determined for the state-specific $OH(X^2\Pi_{1/2}, v'' = 0, J'' = 6.5, 13.5)$ channels were found to be nearly isotropic. The $\mathbf{k} - \mathbf{j}'$ and the $\mathbf{k}' - \mathbf{j}'$ correlations for the $OH(X^2\Pi_{1/2}, v'' = 0, J'' = 13.5)$ showed a broad symmetric distribution with a pronounced maximum at 90°. Recently, the global differential cross section ($\mathbf{k} - \mathbf{k}'$) for the title reaction has been measured using molecular beams,[7] obtaining a quite isotropic distribution with a sharp forward feature. In addition, the reaction of $O(^1D)$ with clusters of ethane[14] and the "half-collision" reaction arising from photodissociation of $C_2H_6 \cdot N_2O$ van der Waals complexes at 193 nm[11] have also been studied.

In this work, we have carried out a full experimental characterization of the internal state distributions of the $OH(X^2\Pi)$ product arising from the $O(^1D) + C_2H_6$ reaction. For the first time, the higher vibrational levels ($v'' = 2-4$) of the OH product for this reaction have been detected at a mean collision energy of 0.52 eV. These results complete previous work performed in our laboratory on the $v'' = 0-1$ levels.[10,12] When these results are compared with those of ref 8 ($\langle E_T \rangle = 0.27$ eV), it is possible to carry out a detailed analysis of the influence of initial collision energy on the dynamical properties of the OH molecules generated in reaction 1, since different enough initial reaction conditions are considered. Moreover, this analysis has allowed us to discuss the microscopic reaction mechanism of the process. Finally, the experimental study of the $O(^1D) + C_2H_6$ reaction has been accompanied by a preliminary theoretical analysis of the nascent OH product energetics corresponding to the $O(^1D) + C_2H_6$ reaction using the quasiclassical trajectory (QCT) method and two pseudotriatomic analytical potential energy surfaces (PESs) developed for the $O(^1D) + CH_4$ reaction.[15,16]

II. Experiment

II.1. Experimental Setup. Experiments were carried out in a laser photolysis LIF setup employing a flow system (Figure 1).[10,12] The experiment includes three steps: (1) initiation of the reaction through the 193 nm photolysis of N_2O; (2) a period of time during which the reaction proceeds; (3) detection of the OH products by means of the LIF technique.

High-purity gases furnished by Praxair were used without further purification (N_2O (99.998%) and C_2H_6 (99.95%)). They were flowed continuously through a stainless steel chamber, which was pumped through a throttled turbomolecular pump (Varian Turbo-1000HT) and a rotary pump (Leybold TRIVAC D40B). With this system, back vacuums of approximately 1×10^{-7} Torr were ordinarily measured using a cold-cathode manometer (Varian senTorr). During an experiment, the gas pressure into the chamber was monitored by a capacitance manometer (Leybold CM1). The total pressure into the chamber and the pumping rate were chosen so that the renewal of the detection volume was allowed between adjacent laser pulses, and thus no residual signal was detected.

The $O(^1D)$ atoms were generated by photodissociation of N_2O at 193 nm using an ArF excimer laser (Lambda-Physik Compex 100). After a fixed time delay controlled with a digital delay generator (Stanford Research DG535), the $OH(X^2\Pi, v'', N'', J'', \Lambda'')$ quantum states arising from the $O(^1D) + C_2H_6$ reaction were probed by LIF in the $A^2\Sigma^+ \leftarrow X^2\Pi$ transition using a XeCl-pumped tunable dye laser (Lambda-Physik LPX 105i and LPD 3002 CES). Both laser beams counterpropagated collinearly; the photolysis laser beam was mildly focused with an $f = 50$ cm fused quartz cell, and the probe laser beam was expanded with a Galilean tellescope.

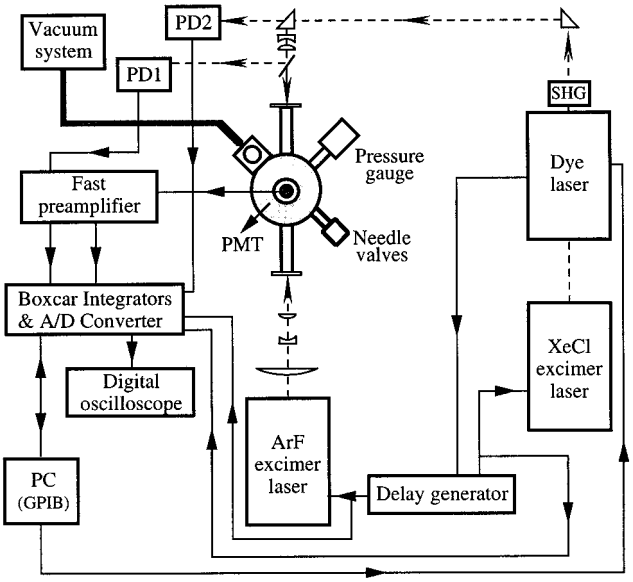

Figure 1. Schematic representation of the experimental setup: (PD1, PD2) photodiodes; (PMT) photomultiplier tube.

The fluorescent emission was collected perpendicularly to the beams' propagation direction through a convergent lens ($f = 75$ mm) and two Oriel UG11 and two Corion SB-300-F filters into a photomultiplier tube (Hamamatsu R1398; PMT in Figure 1). This signal was amplified 5 times in a preamplifier (Stanford SR-240) and sent to two gated integrator boxcars (Stanford SR-250). The first boxcar gate was set to integrate the photolysis laser scattering signal and was used to monitor the photolysis laser power. The second boxcar gate was set to integrate the laser-induced fluorescence decay (LIF signal), and it was triggered by a signal coming from a photodiode (Hamamatsu S1722-02; PD1 in Figure 1), which collects a reflection from the probe laser beam. To monitore the dye laser power, the intensity of another reflection from the probe laser beam is measured by a photodiode (Hamamatsu S1336-5BQ; PD2 in Figure 1) and sent to a third gated boxcar integrator. The three integrated signals coming out from the boxcars were A/D converted (Stanford SR-245) and transferred into a personal computer using a GPIB board. A LabVIEW program developed in our research group[17] was employed to both collect and store the signals from the boxcars (LIF and power signals) and to control the experiment.

The LIF excitation spectra obtained during the experiments were assigned using reported data[18,19] and normalized with respect to the variations in the pump and probe laser powers. Then the area of each peak was measured, and from the normalized areas the populations of the $OH(X^2\Pi, v'', N'', J'', \Lambda'')$ quantum states were extracted using available Einstein B coefficients.[19,20]

To obtain the populations of the $OH(X^2\Pi, v'', N'', J'', \Lambda'')$ states in the $v'' = 0-4$ vibrational levels, the LIF excitation spectra were recorded using the diagonal bands ($\Delta v = 0$), (0,0) and (1,1), and, because of the predissociation of the $A^2\Sigma^+$ state for $N' > 0$ at $v' \geq 2$,[21] the off-diagonal bands ($\Delta v \neq 0$), (0,1), (1,2), (0,2), (1,3), (0,3) and (1,4). Table 1 contains the wave-

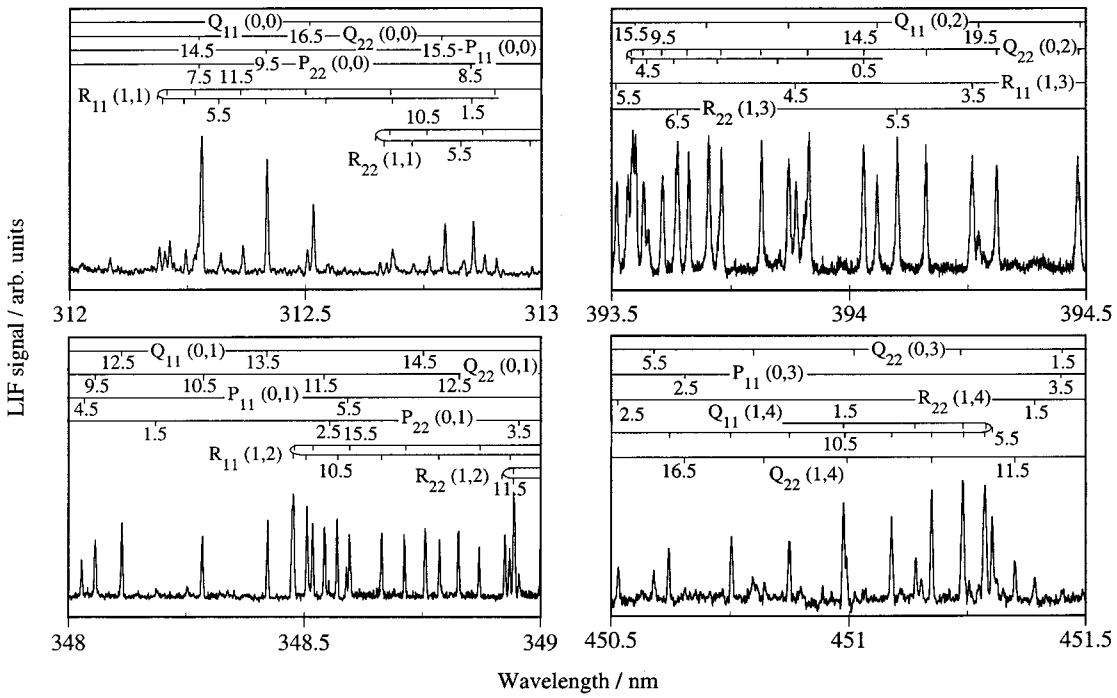

Figure 2. LIF excitation spectra of the nascent OH($X^2\Pi$, $v'' = 0-4$) product arising from the $O(^1D) + C_2H_6$ reaction.

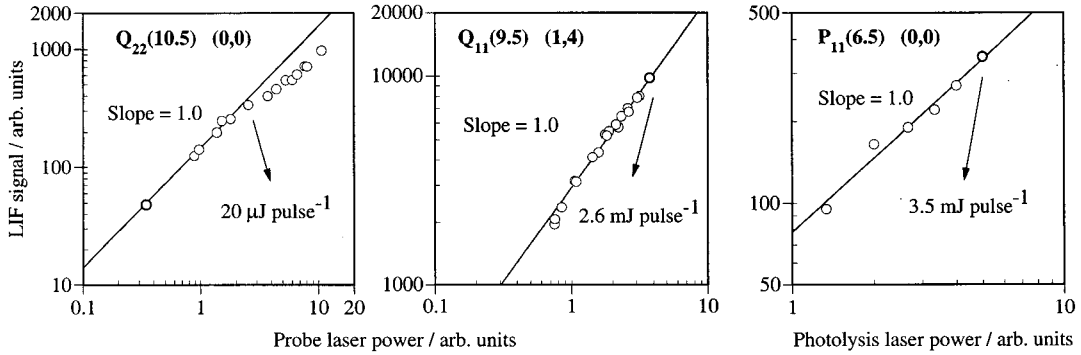

Figure 3. Dependence of the LIF signal with the probe and pump laser powers. The linear correlation between LIF intensity and laser power and the maximum value of the laser power at which this behavior is observed are shown.

TABLE 1: Bands and Dyes Employed in the LIF Detection of OH($X^2\Pi$, $v'' = 0-4$) Molecules

vibrational bands	$\Delta\lambda$/nm	dye solutions
(0,0), (1,1)	306.0−320.0	sulforhodamine B/methanol[a]
(0,1), (1,2)	343.0−358.0	*p*-terphenyl/dioxane and DMQ/dioxane
(0,2), (1,3)	385.0−400.0	QUI/dioxane
(0,3), (1,4)	447.0−460.0	coumarine-120/methanol

[a] To obtain the spectral range required, the output frequency from the dye laser was doubled using a KDP crystal.

length regions scanned and the dyes used in the probe laser for each of these bands. Several examples of LIF excitation spectra for some of the measured bands are given in Figure 2.

II.2. Experimental Conditions. To obtain the nascent distributions of internal states of the OH radical under bulk conditions, the total pressure into the reaction chamber and the delay between the two lasers were kept as low as possible. Thus, typical values of total pressure were 100 mTorr (with an approximate ratio of partial pressures of N_2O and C_2H_6 equal to 1:1), while the laser delay was fixed at 250 ns. It is difficult to establish the amount of vibrational, rotational, spin−orbit, and Λ-doublet deactivation underwent by the nascent OH detected because, to the best of our knowledge, no rate constants for these processes when OH collides with C_2H_6 or N_2O have ever been reported. It has been calculated using a hard-spheres model that, on average, less than 1 collision was suffered by the OH molecules at 100 mTorr and 250 ns conditions before being detected, so it could be expected that there is little effect of state-changing collision processes, even for spin−orbit and Λ-doublet distributions. On the other hand, it has been also calculated following the same procedure that the $O(^1D)$ atoms produced by photolysis underwent less than one collision with other species before reacting. Therefore, it can be expected that the $O(^1D)$ velocity was not significantly reduced by nonreactive collisions, and it could be assumed to be the same one resulting from the photodissociation process.

The population analysis performed in this study relies on the fact that the measurements were made in the linear LIF regime. To confirm that the effect of saturation is negligible, the dependence of the LIF signal with the dye laser power was studied for each of the vibrational LIF bands detected, so the maximum probe laser power at which the LIF spectra could be measured within the linear regime could be established. The results for two of these experiments are given in Figure 3. As might be expected from the values of the Einstein *B* coefficients,[19,20] the linear behavior disappears at higher dye laser power as the $|\Delta v|$

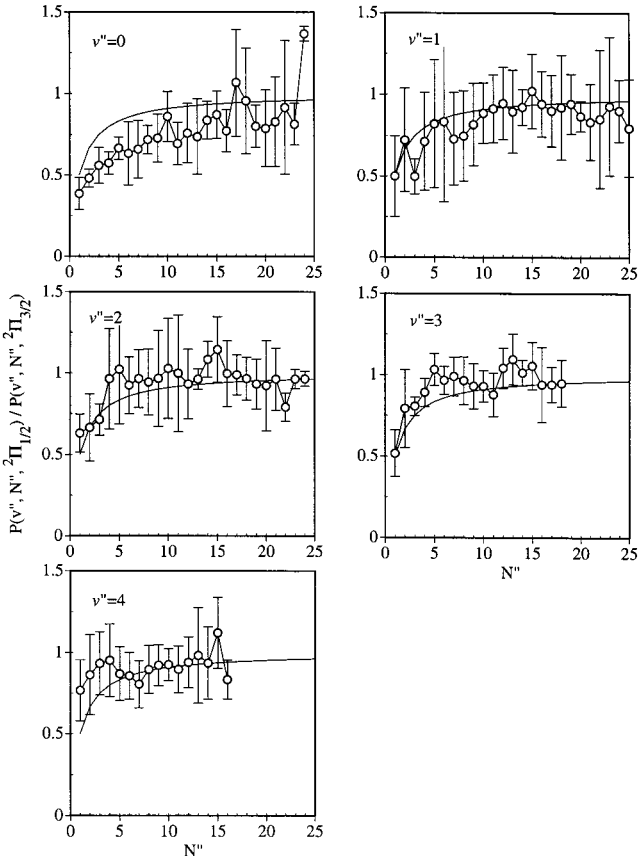

Figure 4. LIF spin−orbit populations ratio (○) for the OH($v''=0-4$) product arising from the $O(^1D) + C_2H_6$ reaction. The line depicted in the graphics corresponds to the statistical population ratio. Error bars correspond to 1 standard deviation.

of the LIF bands increases. The dependence of the LIF intensity with the photolysis laser power was also analyzed. The linear correlation observed indicates that the OH radical is formed only by reaction 1 following the absorption of a single 193 nm photon. Hence, the formation of OH products as a result of processes that imply the absorption of zero or more than one 193 nm photons could be discarded.

II.3. Experimental Results. *II.3.A. Spin−Orbit and Λ-Doublet Populations.* The spin−orbit interaction in OH($X^2\Pi$) leads to the existence of two electronic fine structure states, F_1 and F_2 ($X^2\Pi_{3/2}$ and $X^2\Pi_{1/2}$, respectively), whose population in the statistical limit only depends on their degeneracy. Thus, the statistical population ratio between both spin−orbit states, $P(F_1)/P(F_2)$, should be equal to $(N''+1)/N''$ for each rotational level. Figure 4 shows the experimental and the statistical limit spin−orbit populations ratio, $P(v'',N'',X^2\Pi_{1/2})/P(v'',N'',X^2\Pi_{3/2})$, as a function of N''. Table 2 collects the average $[P(v'',N'',X^2\Pi_{3/2})N''/(P(v'',N'',X^2\Pi_{1/2})(N''+1))]$ ratios obtained for OH($X^2\Pi$, $v''=0-4$). Considering the confidence intervals of the measurements, it can be stated that there is no preferential population of any of the two spin−orbit states. The same results were reported in previous studies on reaction 1 at $\langle E_T\rangle = 0.27$ eV[8] for $v''=0-4$ and at $\langle E_T\rangle = 0.52$ eV[10−12] for $v''=0-1$.

Two Λ-doublet fine structure states, Π(A′) and Π(A″), arise from the interaction of electronic orbital and rotational angular momenta. In the high rotational levels limit case, the Π(A′) state corresponds to the alignment of the half-filled π OH molecular orbital in the rotation plane, while a perpendicular alignment of this orbital to that plane occurs for the Π(A″) state. Figure 5 shows the Λ-doublet populations ratio $P(\Pi(A'))/P(\Pi(A''))$ as a function of N''. Table 2 collects the average values for

TABLE 2: Average Spin−Orbit Populations Ratio $[P(v'',N'',X^2\Pi_{3/2})N'']/[P(v'',N'',X^2\Pi_{1/2})(N''+1)]$ and Average Λ-Doublet Populations Ratio $P(\Pi(A'))/P(\Pi(A''))$ for OH($X^2\Pi$, $v''=0-4$) Molecules Arising from Reaction 1

v''	$[P(v'',X^2\Pi_{3/2})N'']/[P(v'',X^2\Pi_{1/2})(N''+1)]$[a]	$P(v'',\Pi(A'))/P(v'',\Pi(A''))$[a]
0	1.18 ± 0.25	1.43 ± 0.29
1	1.04 ± 0.22	1.34 ± 0.32
2	0.94 ± 0.21	1.14 ± 0.22
3	0.93 ± 0.13	1.23 ± 0.18
4	0.96 ± 0.18	1.29 ± 0.27
all v''[b]	1.07 ± 0.22	1.33 ± 0.27

[a] The statistical ratio values are always equal to 1. [b] Averaged over all v'' levels, considering each level population.

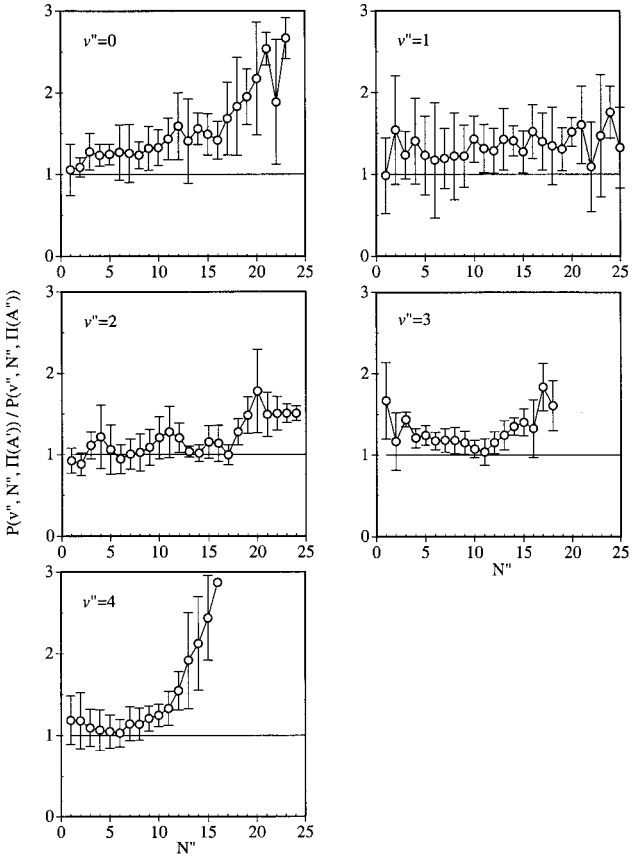

Figure 5. LIF Λ-doubling populations ratio (○) for the OH($v''=0-4$) product arising from the $O(^1D) + C_2H_6$ reaction. The line depicted in the graphics corresponds to the statistical population ratio. Error bars correspond to 1 standard deviation.

$v''=0-4$. These results show a preferential population of the Π(A′) state. This fact is usually explained on the basis of an insertion-type reaction mechanism where the OH rotation follows a preferential orientation during the fragmentation of the R−O−H bent collision complex. The same results were reported in previous studies on reaction 1 at $\langle E_T\rangle = 0.27$ eV[8] for $v''=0-4$ and at $\langle E_T\rangle = 0.52$ eV[10−12] for $v''=0-1$.

II.3.B. Rotational Distributions. Figure 6 depicts the experimentally measured nascent OH($X^2\Pi$, $v''=0-4$) product rotational distributions arising from reaction 1. The average rotational levels for each of the vibrational levels populated are given in Table 3. From Figure 6 it might be stated that the measured rotational distribution for $v''=0$ is quite different from the remaining ones. Thus, the rotational distribution obtained for $v''=0$ is clearly bimodal, presenting a predominant component peaked at low-N'' values and a second component

TABLE 3: Average Rotational Levels of the OH($X^2\Pi$, $v'' = 0-4$) Rotational Distributions Arising from Reaction 1 and Characteristic Properties[a] of the High-N'' and Low-N'' Components of These Distributions

		experimental values[b]				
		$v'' = 0$	$v'' = 1$	$v'' = 2$	$v'' = 3$	$v'' = 4$
$\langle N'' \rangle_{v''}$	this work	10.5 ± 0.2	13.0 ± 0.4	11.6 ± 0.3	9.3 ± 0.2	7.9 ± 0.2
	ref 8	9.9	12.6	10.0	7.9	5.3
$P_{low-N''}/P_{high-N''}$	this work	0.56	0.02	0.00	0.00	0.12
	ref 8	0.75	0.11	0.00	0.00	0.00
$-\theta_R$	this work	11.8	11.0	8.7	6.6	5.2
	ref 8	10.6	8.9	7.2	5.4	2.3
T/K	this work	885				470
	ref 8	795				

[a] The characteristic properties are the yield ratio between the low-N'' and high-N'' components ($P_{low-N''}/P_{high-N''}$), the slope of the high-N'' component in the surprisal plot (θ_R), and the temperature derived by fitting a Maxwell−Boltzmann distribution to the low-N'' component (T). [b] $\langle E_T \rangle = 0.52$ and 0.27 eV for this work and ref 8, respectively. The average rotational levels and the temperature value given for ref 8 have been derived from the rotational distributions depicted in that work.

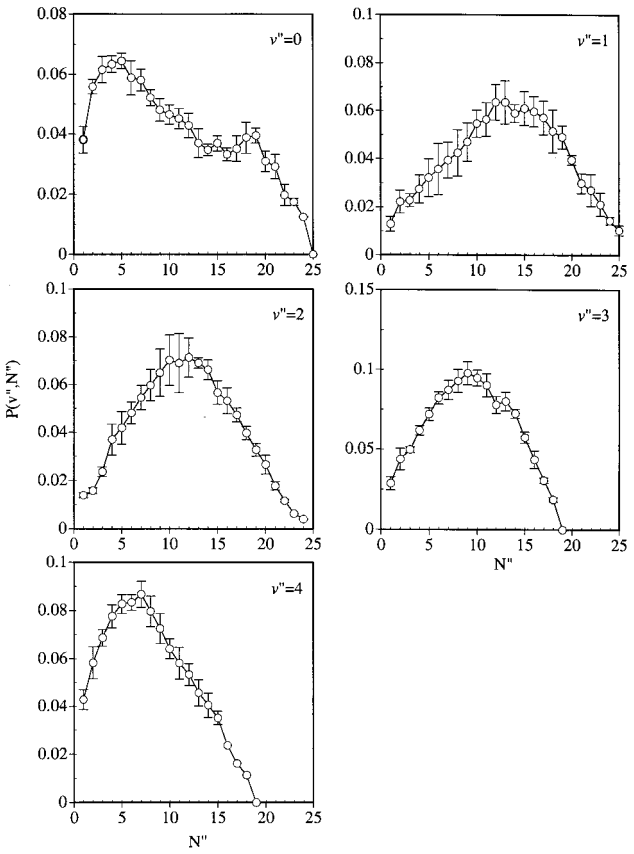

Figure 6. LIF rotational populations (○) for the OH($v'' = 0-4$) product arising from the $O(^1D) + C_2H_6$ reaction. Error bars correspond to 1 standard deviation. Populations are normalized to unity.

reaching higher rotational levels. The rotational distributions for vibrational levels $v'' > 0$, however, seem to be essentially unimodal with a maximum that appears at high-N'' levels, its value diminishing as the vibrational quantum number increases, as generally expected.

The qualitative analysis of Figure 6 can be put on a quantitative basis by carrying out a surprisal analysis of the rotational distributions.[8,22] Essentially, this method evaluates the degree of deviation of the experimental distributions ($P(v'',N'')$) from the prior one ($P^0(v'',N'')$).[23] To deal with this, the rotational surprisal, I_R ($I_R = -\ln[P(v'',N'')/P^0(v'',N'')]$), is plotted as a function of the g_R parameter ($g_R = f_r/(1 - f_v)$), which is expressed in terms of the fractions of available energy disposed in OH rotation (f_r) and vibration (f_v). In Figure 7 the surprisal plots derived for OH($X^2\Pi$, $v'' = 0$, 2, 4) are collected. As can be observed, the surprisal plot derived for OH($X^2\Pi$, $v'' = 0$) clearly deviates from the ones obtained for higher vibrational levels. In that case, there is a clear bimodal behavior because the surprisal plot presents a negative slope at low-N'' values and a positive slope at high-N'' values, each one of them reflecting the two components previously observed in the rotational distribution plot (low-N'' and high-N'' components). On the other hand, the surprisal plots for OH($v'' = 1-3$) show a single component with a positive slope (resembling the high-N'' component observed for $v'' = 0$) ranging over all the measured N'', as can be observed in the surprisal plot depicted in Figure 7 for OH($X^2\Pi$, $v'' = 2$). In regard to the surprisal analysis performed for $v'' = 4$, even though it shows the existence of a major contribution of the high-N'' component to the rotational distribution, the surprisal plot obtained in this case somewhat resembles the one derived for $v'' = 0$ because it also has a small negative slope region at low-N'' values (Figure 7).

From the surprisal analysis, the contributions of the high-N'' and low-N'' components detected in the OH rotational distributions have been determined. The values obtained are shown in Table 3, and as above-mentioned they indicate that the low-N'' component only contributes significantly to the rotational distributions of the OH product for the $v'' = 0$ level, with also a nonnegligible contribution in the case of $v'' = 4$. The characteristic slopes (θ_R) of the high-N'' components and the temperatures derived by the fitting of the low-N'' components for OH($X^2\Pi$, $v'' = 0$, 4) by Maxwell−Boltzmann distributions are also given in Table 3.

Each of the different components observed in the OH product rotational distributions can be assigned to different possible microscopic mechanisms for reaction 1. The large negative values found for the θ_R parameter of the high-N'' components indicate the existence of much more rotational excitation than expected. This fact suggests that this rotational component may arise from the dissociation of a highly energized CH_3CH_2OH collision complex prior to redistribution of the available energy in that complex through energy transfer among its internal degrees of freedom.[8−12] Therefore, a microscopic mechanism evolving through the insertion of an $O(^1D)$ atom into a C−H bond to yield an alcohol-type collision complex followed by a fast elimination of the OH molecule can be assigned to the production of the high-N'' component. On the other hand, the little rotational excitation associated with the low-N'' component observed for OH($X^2\Pi$, $v'' = 0$) suggests that this component may arise from the dissociation of a quite stabilized CH_3CH_2-OH collision complex.[8,10−12] Thus, the low-N'' rotational component can be assigned to an insertion mechanism followed

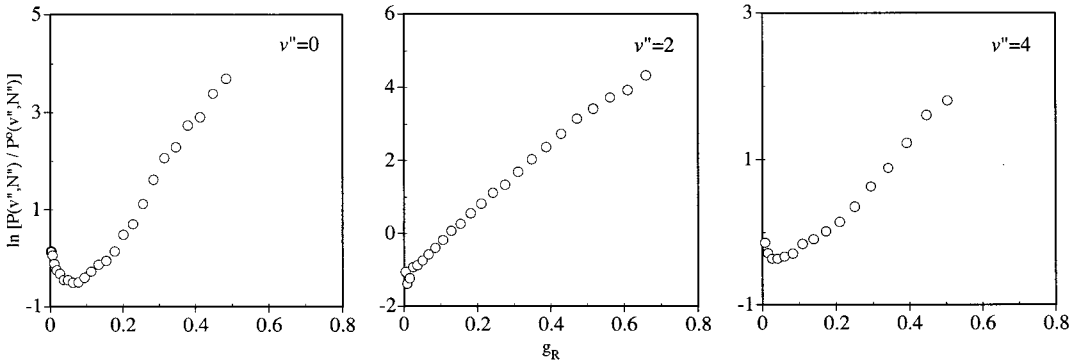

Figure 7. LIF rotational surprisals plots (○) for the OH(v'' = 0, 2, 4) product arising from the O(1D) + C_2H_6 reaction.

by a slow elimination of OH through a long-lived collision complex. In this case little vibrational excitation should be expected for the OH product, this fact explaining the negligible contribution observed for the low-N'' component at higher vibrational levels.

As a consequence of the above-indicated considerations, the low-N'' component detected in the case of $v'' = 4$ cannot be associated with the same reaction mode assigned for the low-N'' component in OH($v'' = 0$). In principle, that rotational component might be due to the existence of relaxation effects by collision. This would make the affected distributions be shifted toward low-N" values, then leading to a spurious low-N'' component in the rotational surprisal plots. However, because no relaxation effects by collision are observed in the rotational distributions for lower vibrational levels of the OH product, the use of such an explanation to justify the behavior detected for the rotational distribution of OH($v'' = 4$) may be rejected. Therefore, the low-N'' component in $v'' = 4$ may arise from the existence of a microscopic reaction mechanism different from the ones already introduced (insertion/fast elimination and insertion/slow elimination). In fact, the features established for the low-N'' component in OH($v'' = 4$) (little rotational and high vibrational excitation) are closer to what should be expected for large exothermic processes like reaction 1 when they evolve through an abstraction mechanism. In the case of reaction 1 this kind of direct microscopic mechanism corresponds to the abstraction of an H atom of the hydrocarbon by the attacking oxygen.

Despite the conclusion in the previous paragraph, it is recognized that the experimental indications found in the present work about the contribution of the abstraction mechanism (the bimodal feature in the OH($v'' = 4$) surprisal plot) are not fully conclusive. However, at this point it is important to mention the results obtained by us in a recent study of the OH product energetics arising from the analogous O(1D) + C_2H_4 reaction.[24] For this system, similar behavior with respect to the title reaction in regard to the final energetics of the OH product[24,25] and its stereodynamics[13] has been reported, the CC double bond playing a minor role. Thus, it can be expected that both processes occur via the same reaction mechanism. Then the clear bimodal feature reported for the OH($v'' = 3$) product arising from the reaction with ethylene[24] (this is the highest populated vibrational level in this case) supports the experimental evidence found for the title reaction and reinforces the suggestion that for this kind of system an abstraction mechanism plays a nonnegligible role in the formation of OH molecules in the highest vibrational states.

The abstraction mechanism could proceed through different ways. Thus, this reaction mode could take place directly on the ground potential energy surface (1^{1}A PES) of the O(1D) + C_2H_6 system, arising as a competitive reaction mode to the insertion pathways. For the related O(1D) + $CH_4 \rightarrow$ OH + CH_3 reaction, such a situation was suggested from ab initio calculations[26] of the ground PES and shown later in dynamical studies[15,16] of it. It was reported in refs 15 and 16 that an abstraction mechanism evolving through the ground 1^{1}A potential energy surface, which has a global contribution to the reactivity smaller than 1−2%, yielded the formation of high vibrationally excited (the population maximum appeared at $v'' = 4$) and low rotationally excited OH molecules. As will be shown in section III.B, similar results have been obtained when applying the quasiclassical trajectory method for the description of the O(1D) + C_2H_6 reaction.

On the other hand, the abstraction mechanism may also occur in the first excited surface (2^{1}A PES) of the O(1D) + C_2H_6 system. Some high level ab initio calculations still in progress in our group show that the energy barrier corresponding to the first excited PES for the O(1D) + CH_4 reaction is around 1−2 kcal mol^{-1} and that it connects reactants with the OH + CH_3 products through an abstraction reaction pathway.[27] Therefore, the possibility that the 2^{1}A PES contributed appreciably to the reactivity of the O(1D) + hydrocarbon systems at the values of E_T usually employed in the experiments cannot be discarded. If this situation was attained, then the reactive behavior of these systems would somewhat resemble the one established for the O(1D) + $H_2 \rightarrow$ OH + H reaction. For this process and its deuterated isotopic variants, both experimental (see, for example, refs 28−30) and theoretical (see, for example, refs 31−34) studies have shown that although the major contribution to the reactivity is due to a fast insertion/elimination mechanism, which evolves through the ground 1^{1}A′ PES, the low-energy barrier that presents the first excited potential energy surface (1^{1}A″ PES) allows an abstraction reaction mechanism to take place on it, yielding high vibrationally and low rotationally excited OH molecules.

As a matter of fact, in a very recent contribution,[35] the OH($X^2\Pi$, $v'' = 3$, 4) rovibrational distributions arising from the O(1D) + H_2 reaction were experimentally measured and also theoretically calculated using rigorous quantum dynamical calculations on high-quality analytical representations of the ground and first excited PESs of the system. It was observed that, although the OH($v'' = 4$) rotational distribution was apparently unimodal, the abstraction mechanism evolving through the excited PES contributed in a significant extent (approximately 20%) to the formation of the OH($v'' = 4$) molecules (but not for the $v'' = 3$ or lower levels), this mechanism yielding less rotational excitation than the one occurring via the ground PES. In fact, it was found that the experimental OH($v''=4$) rotational distribution and $P(v''=4)$/$P(v''=3)$ vibrational populations ratio were excellently reproduced when considering both the insertion/elimination mech-

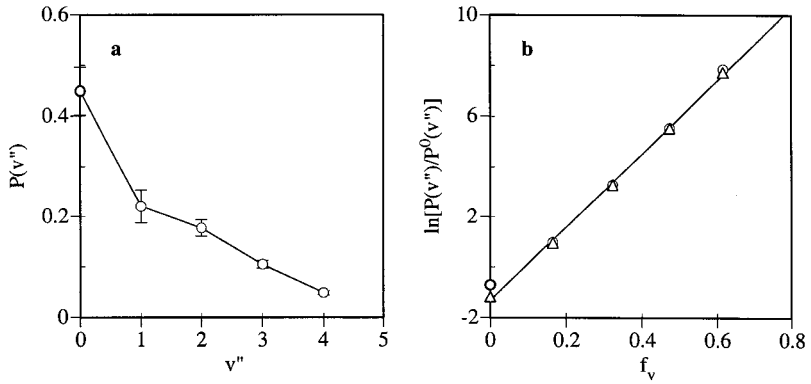

Figure 8. (a) LIF vibrational populations (○) for the OH($v''=0-4$) product arising from the O(^{1}D) + C_2H_6 reaction. Error bars correspond to 1 standard deviation. Populations are normalized to unity. (b) Vibrational surprisals plots for the global vibrational populations (○) and for the vibrational populations corresponding to the high-N'' rotational component (△).

TABLE 4: Vibrational Populations for the OH($X^2\Pi$, $v''=0-4$) Molecules Arising from Reaction 1

		$P(v'')/P(v''=1)$				
study	$\langle E_T\rangle$/eV	$v''=0$	$v''=1$	$v''=2$	$v''=3$	$v''=4$
this work	0.52	2.04 ± 0.51	1.00	0.80 ± 0.19	0.48 ± 0.10	0.22 ± 0.05
ref 8	0.27	2.50	1.00	0.70	0.43	0.38

anism (evolving through the ground PES) and the abstraction one (occurring through the excited surface).

Finally, in early studies of the O(^{1}D) + hydrocarbon reactions,[9] it was stated that an abstraction mechanism could also occur via intersystem crossing between the ground PESs of the O(^{1}D) + hydrocarbon (1^1A PES) and O(^{3}P) + hydrocarbon (1^3A PES) systems. However, in a recent study of the transitions between the singlet and triplet surfaces of the related O + H_2 system, it has been found that the contribution of the intersystem crossing to the reactivity of the O(^{1}D) + H_2 process is negligible.[36] Moreover, LIF measurements[37,38] and QCT calculations[39,40] about the OH product arising from the O(^{3}P) + saturated hydrocarbon reactions have shown that internally cold OH molecules with a preferential population of the $^2\Pi_{3/2}$ spin−orbit state are produced by a direct abstraction mechanism on the ground triplet surface of these systems, these findings differing from what has been observed for the low-N'' component of OH($v''=4$) arising from the O(^{1}D) + C_2H_6 process. Nevertheless, different properties may be expected for the OH product when it is produced on the 1^3A PES under intersystem crossing conditions.

The rotational distributions obtained in this work at $\langle E_T\rangle = 0.52$ eV have been compared with those obtained in the previous full characterization of the energetics of OH product arising from reaction 1 at $\langle E_T\rangle = 0.27$ eV.[8] No strong differences have been found between both kind of results, probably because of the large reaction exothermicity, which attenuates the influence of the initial reaction conditions on the dynamics (the products available energy is equal to 2.40 and 2.65 eV for $\langle E_T\rangle = 0.27$ and 0.52 eV, respectively). Moreover, the fact that similar results were obtained in both studies of the energetics of the OH product is useful information because it reinforces the suggestion that the process mainly evolves through an insertion/elimination mechanism, since this reaction mode should be expected to be little sensitive to changes in collision energy. The predominance of this kind of insertion/elimination reaction mode has also been indicated by the experiments on the stereodynamics of reaction 1.[7,13]

However, if a deeper analysis of the results is performed, it must be noted that the rotational distributions obtained at $\langle E_T\rangle = 0.52$ eV are somewhat more excited than the corresponding ones at $\langle E_T\rangle = 0.27$ eV and that the enhancement of the rotational excitation is stressed as higher OH vibrational levels are considered. This situation is evidenced by the average rotational levels given in Table 3. Moreover, it can also be observed that the high-N'' component for OH($X^2\Pi$, $v''=0-1$) is more populated at $\langle E_T\rangle = 0.52$ eV, and for this reaction condition more negative values of the θ_R parameter are obtained. These facts indicate that increasing collision energy not only favors the fast elimination of products (the high-N'' component) but also leads to somewhat higher rotational excitation of the fast-eliminated OH molecules. On the other hand, the low-N'' components corresponding to OH($X^2\Pi$, $v''=0$) are very similar for both reaction conditions, thus supporting the statement that this component may arise from dissociation of long-lived collision complexes, because this microscopic mechanism might show a smaller dependence on the initial translational energy.

In the experimental study performed at $\langle E_T\rangle = 0.27$ eV, no evidence for bimodal behavior of the OH($v''=4$) rotational distribution[8] was reported and it was indicated that this distribution only shows the contribution of the high-N'' component. However, the shape of the rotational distribution depicted in ref 8 for OH($v''=4$) is very similar to the one obtained in this work. This distribution was less excited than the essentially unimodal ones for OH($v''=1-3$) and it was shifted toward lower values of N''. Anyway, if it is assumed that the low-N'' component observed in the present work for the rotational distribution at $v''=4$ arises from an abstraction-type mechanism, it may be expected that the contribution of this reaction mode does change significantly with collision energy. The higher the collision energy is, the larger the contribution of the abstraction mechanism should be, because an energy barrier controls the evolution through this direct mechanism. Therefore, the contribution of this mechanism at $\langle E_T\rangle = 0.27$ eV could be much too small to be detected experimentally.

II.3.C. Vibrational Populations. The population of each OH($X^2\Pi$) vibrational level arising from reaction 1 has been determined by summing up the rotational populations measured. The vibrational populations obtained for OH($X^2\Pi$, $v''=0-4$) are given in Table 4, and they are drawn in Figure 8a.

The analysis of the vibrational populations measured has been performed in terms of the vibrational surprisals,[8,22,23] I_v ($I_v = -\ln[P(v'')/P^0(v'')]$), which were plotted as a function of the average fraction of available energy released as vibrational energy of OH product (f_v) (Figure 8b). The graphic derived shows nonlinear behavior principally due to the population value at $v'' = 0$. If the vibrational surprisal analysis is only carried out for the vibrational populations associated with the high-N'' component, then the existence of a linear correlation is verified. Such a behavior reinforces the suggestion that this component arises from a single mechanism. Moreover, it must be pointed out that the linear behavior obtained for the vibrational surprisal analysis of the high-N'' component displays large negative values of λ_v ($\lambda_v = dI_v/df_v$), which implies that the high-N'' contribution might be due to a strongly nonstatistical process, as the mechanism of insertion/fast elimination is. On the other hand, the subtraction of the low-N'' component contribution from the global vibrational population for $v'' = 4$ to obtain the high-N'' component population also allows for a better linear correlation in the surprisal plot, just as it has also been observed in our recent contribution to the related O(^{1}D) + C_2H_4 system.[24] This fact supports the suggestion that a nonnegligible amount of the OH($v'' = 4$) molecules are being produced by a different mechanism than the insertion/fast elimination mechanism, that is to say, by an abstraction mechanism. However, because the contribution of the abstraction reaction mode is really small, the break of the linear correlation in the surprisal plot for the $v'' = 4$ level due to this reaction mode is not highly evident.

The OH vibrational distribution measured in this work at $\langle E_T \rangle = 0.52$ eV has been compared with the one reported in ref 8 at $\langle E_T \rangle = 0.27$ eV. As was observed for the rotational distributions, there are no large differences between the vibrational distributions obtained for both conditions (see Table 4). This can be rationalized in terms of the influence of the large exothermicity of the O(^{1}D) + C_2H_6 reaction and also in terms of the presence of a deep minimum through which the reactivity mainly evolves. However, it must be noted that a slight increase of the OH vibrational excitation is found with rising the collision energy, as was commented above regarding the OH rotation.

When the vibrational surprisal analysis was performed in ref 8, a linear correlation for the high-N'' component was also obtained. However, the data corresponding to the $v'' = 4$ vibrational level slightly deviate from linear behavior, indicating that the population of the high-N'' component in $v'' = 4$ could be somewhat overestimated. This fact may suggest that some of the population assigned to the high-N'' component in this vibrational level (and therefore corresponding to the insertion/fast elimination mechanism) belongs to another rotational component (and therefore to another mechanism), as has been concluded in the present work.

III. Theory

III.1. Theoretical Methodology. To perform a complementary theoretical study of the O(^{1}D) + $C_2H_6 \rightarrow$ OH + C_2H_5 reaction, the two ab initio based analytical triatomic potential energy surfaces (PES1 and PES2) previously derived in our group for the analogous reaction between O(^{1}D) and CH_4 were used (see refs 15 and 16 for further details). In these PESs the methyl group was treated as a pseudoatom of 15 amu. Both PESs are quite similar, although PES1 exhibits a small barrier along the minimum energy path and PES2 is a barrierless surface. In general, the use of any of these two analytical PESs versions of the ground potential energy surface (1^1A in C_1 symmetry) of the O(^{1}D) + CH_4 system allowed us to obtain a rather good reproduction of its dynamics behavior, not only concerning the OH product final energetics but also concerning other detailed properties (state-specific differential cross sections ($\mathbf{k} - \mathbf{k}'$) and product translational energy distributions).[12,15,16] This was possible because the two PESs were found to be especially efficient in describing the insertion/fast elimination mechanism that is believed to be the most important one for the O(^{1}D) + hydrocarbon reactions. However, the consideration of a triatomic model treating the CH_3 group as a pseudoatom led to a relatively poor description of the insertion/slow elimination mechanism, for which the energy transfer to the internal degrees of freedom of the methyl group could not be neglected.

According to the similarities between the reactions of O(^{1}D) atoms with either methane or ethane and disregarding the presence of a C−C bond in ethane, it may be expected that the insertion/fast elimination mechanism corresponding to reaction 1 could also be rather well reproduced using PES1 and PES2. This is the reason that the same procedure (QCT method[15,16,40−42]) and potential energy surfaces (PES1 and PES2) that were employed previously to analyze the O(^{1}D) + CH_4 system have been applied here to study reaction 1. In this case, the mass of the pseudoatom used in the QCT calculations on PES1 and PES2 has been taken as the mass of the C_2H_5 group (29 amu). Moreover, this theoretical study has been centered in those properties corresponding to the insertion/fast elimination mechanism. This was achieved by just analyzing the properties of the corresponding reactive trajectories, as was described in our previous contributions on the O(^{1}D) + CH_4 system.[15,16]

III.2. Theoretical Results. The nascent OH($X^2\Pi$, $v'' = 0-4$) rovibrational distributions corresponding to the insertion/ fast elimination mechanism of the O(^{1}D) + $C_2H_6 \rightarrow$ OH + C_2H_5 reaction have been calculated by applying the QCT method on both PES1 and PES2 for E_T values of 0.27 and 0.52 eV. In Figure 9, the vibrational distributions found at $E_T = 0.27$ and 0.52 eV are compared with the experimental ones reported in this work ($\langle E_T \rangle = 0.52$ eV) and in ref 8 ($\langle E_T \rangle = 0.27$ eV) for that microscopic mechanism. In Figures 10 and 11, the comparison between the experimental and theoretical rotational distributions at E_T=0.27 and 0.52 eV, respectively, is given.

The QCT vibrational distributions depicted in Figure 9 does not exactly fit the experimental results at $\langle E_T \rangle = 0.27$ eV or at $\langle E_T \rangle = 0.52$ eV, providing more OH vibrational excitation than the experiments. The average vibrational levels derived for the calculations are $\langle v'' \rangle = 2.0$ (PES1) and 1.6 (PES2) at $E_T = 0.27$ eV and $\langle v'' \rangle = 2.0$ (PES1) and 1.8 (PES2) at $E_T = 0.52$ eV, while the experimentally obtained values are $\langle v'' \rangle = 1.2$ ($\langle E_T \rangle = 0.27$ eV) and 1.3 ($\langle E_T \rangle = 0.52$ eV). Nevertheless, the distributions obtained for PES2 qualitatively reproduce the experimental data at both collision energies, showing a monotonic decrease of the vibrational population as the vibrational quantum number increases. For the distributions for PES1, they suggest the existence of much more vibrational excitation than in the experimental results because the PES1 vibrational distributions obtained were inverted and their population maxima appeared at $v'' = 2$. The different behavior obtained for the two PESs can be rationalized on the basis of their different topologies. Thus, as above-mentioned, PES1 presents a small barrier in the entrance channel of the reaction as a consequence of the triatomic model used, while PES2 was forced to be barrierless in order to reproduce the experimental information about the rate constant.[15,16] In principle, it might be expected

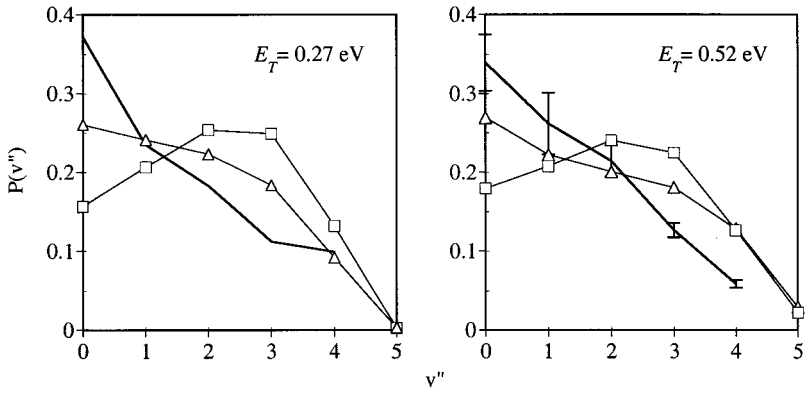

Figure 9. LIF (−) and QCT (□, PES1; △, PES2) vibrational distributions for the OH($v'' = 0-4$) product arising from the insertion/fast elimination mechanism associated with the $O(^1D) + C_2H_6$ reaction at $E_T = 0.27$ (LIF data from ref 8) and 0.52 eV (the present work). Populations are normalized to unity.

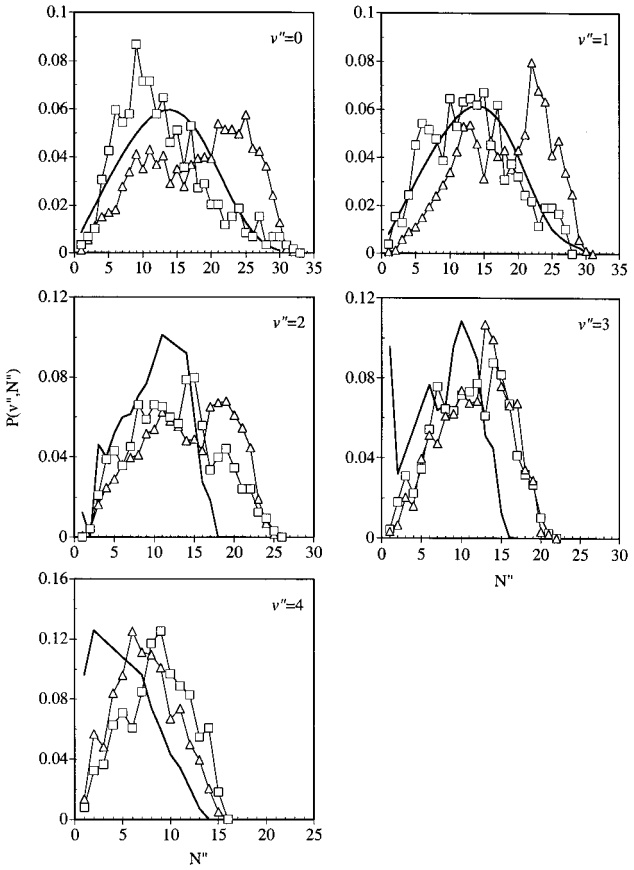

Figure 10. LIF (−) and QCT (□, PES1; △, PES2) rotational distributions for the OH($v'' = 0-4$) product arising from the insertion/fast elimination mechanism associated with the $O(^1D) + C_2H_6$ reaction at $E_T = 0.27$ eV (LIF data from ref 8). Populations are normalized to unity.

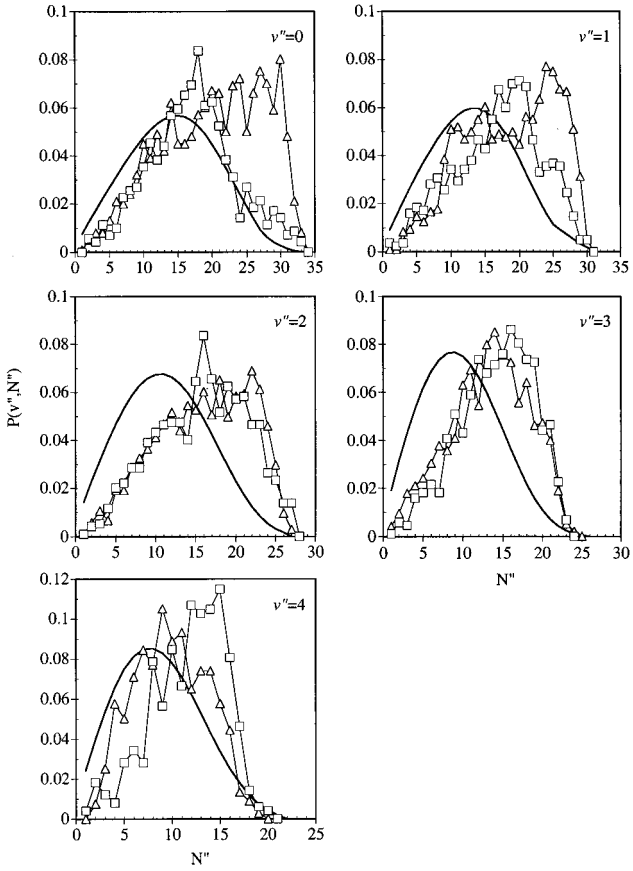

Figure 11. LIF (−) and QCT (□, PES1; △, PES2) rotational distributions for the OH($v'' = 0-4$) product arising from the insertion/fast elimination mechanism associated with the $O(^1D) + C_2H_6$ reaction at $E_T = 0.52$ eV (the present work). Populations are normalized to unity.

that the presence of the early barrier in PES1 favors more vibrational excitation of the OH product.

The theoretical rotational distributions reproduce quite well the shape of the experimental distributions, specially for $E_T = 0.27$ eV, as can be observed in Figure 10. However, the calculations yield more rotational excitation than experimentally found, especially for $E_T = 0.52$ eV, as can be appreciated in Figure 11. Thus, the average rotational levels derived from QCT results are in general about 3−4 rotational quantum numbers higher than the experimental values. In this case, it must be noted that PES1 provides better results than PES2 (essentially for $v'' = 0-1$), unlike what was observed for the vibration. The differences of both PESs in the entry channel together with the subtle differences that are exhibited in the exit channel should account for their different behavior regarding the OH rotation results.

The differences detected between the experimental data and the theoretical results for both the vibrational and rotational distributions are not too important if the kind of approximations that have been included in the calculations is taken into account. As a matter of fact, the experimental behavior of the insertion/fast elimination mechanism studied is qualitatively well-reproduced by the theoretical calculations, thus concluding that this reaction mode may not differ in an important extent from the analogous one for the $O(^1D) + CH_4 \rightarrow OH + CH_3$ reaction. That is to say, the additional complexity introduced by the

presence of a C−C bond in ethane does not involve significant changes regarding the insertion/fast elimination microscopic mechanism of reaction 1.

The occurrence of abstraction-like reactive trajectories in the QCT calculations on the ground PES of the $O(^1D) + C_2H_6$ reaction has also been studied. To deal with this, the minimal value of the PES energy reached by each reactive trajectory was analyzed (the PES energies at the equilibrium geometries of reactants, products, and $(C_2H_5)OH$ minimum are, respectively, −4.79, −6.47, and −10.56 (PES1) and −10.54 (PES2) eV, where the zero of energy corresponds to $O(^1D) + H + (C_2H_5)$). In this way, it was found that about 1−2% of the reactive trajectories evolved from reactants to products with a minimum PES energy higher than −6.5 eV. All remaining trajectories took values below −9.0 eV. An analysis of the temporal evolution of the interatomic distances allowed us to unambiguously assign the former trajectories to an abstraction mechanism, while the latter ones were ascribed to insertion. Similar results were also obtained in our previous theoretical studies of the $O(^1D) + CH_4$ reaction.[15,16]

The properties established for the abstraction-like trajectories also support the experimental evidence for this mechanism shown in section II. Thus, the OH vibrational populations (normalized to unity) found for the abstraction mechanism at $E_T = 0.52$ eV and using PES2 are $P(v''=0) = 0$, $P(v''=1) = 0$, $P(v''=2) = 0.01$, $P(v''=3) = 0.06$, $P(v''=4) = 0.51$, and $P(v''=5) = 0.42$. Similar results were also obtained with PES1. Hence, as experimentally suggested, a nonnegligible contribution of the abstraction mechanism should be expected for $OH(v'' \geq 4)$. In fact, according to the QCT calculations, the abstraction mechanism approximately accounts for the 10% and 30% of the $OH(v' = 4)$ and $OH(v' = 5)$ molecules produced, respectively. Regarding the rotational distributions for this reaction mode, there is not enough statistics to infer quantitative conclusions. However, it seems that for the $OH(v'' = 4)$ molecules, the rotational distribution for abstraction is less excited than the insertion/fast elimination one, which would account for the bimodal feature experimentally observed.

IV. Summary and Conclusions

The full characterization of the nascent $OH(X^2\Pi, v'', N'', J'', \Lambda'')$ product state distributions for the $O(^1D) + C_2H_6 \rightarrow OH + C_2H_5$ reaction has been experimentally performed using the LIF technique to probe the $v'' = 0-4$ levels of the OH molecules. This thorough study has been carried out for the first time using the N_2O photodissociation at 193 nm to generate the $O(^1D)$ atoms ($\langle E_T \rangle = 0.52$ eV), thus not only completing the previous preliminary study of the $v'' = 0-1$ levels at this reaction condition[10−12] but also allowing for a comprehensive analysis of the influence of the collision energy on the dynamics of this process by comparison with the experimental available data for $\langle E_T \rangle = 0.27$ eV[8] and also by taking into account QCT results from model triatomic PESs. In this way, a discussion about the microscopic mechanism of the title reaction can be carried out.

The results obtained in this work suggest the existence of a small effect of E_T on the dynamics of the $O(^1D) + C_2H_6 \rightarrow OH + C_2H_5$ reaction. The spin−orbit distributions of the OH product show a statistical population of the $^2\Pi_{3/2}$ and $^2\Pi_{1/2}$ states, while some preference for the formation of the $\Pi(A')$ Λ-doublet state has been detected, as reported in ref 8. Only somewhat higher rovibrational excitation of the OH product has been observed on increasing the collision energy of the system, which indicates that the large exothermicity of the $O(^1D) + C_2H_6$ process and the presence of a deep alcohol minimum on the PES through which the reaction mainly takes place via an insertion/elimination mechanism soften the changes on E_T. Thus, the available energy of the products is equal to 2.40 and 2.65 eV for $\langle E_T \rangle = 0.27$ and 0.52 eV, respectively.

A comparison between the results obtained in this work and those reported in ref 8 supports the belief that the studied reaction essentially evolves through the insertion of the $O(^1D)$ atom into a C−H bond, yielding both short-lived (fast elimination) and long-lived (slow elimination) collision complexes. However, although not fully conclusive, some evidence has been found on the coexistence of a third microscopic reaction mechanism (abstraction), which may contribute to the formation of the highest vibrationally excited OH molecules with low rotational excitation. The possible contribution of the abstraction mechanism is additionally supported by very recent measurements performed by us on the analogous $O(^1D) + C_2H_4$ reaction and by theoretical and experimental data of other authors on the related $O(^1D) + H_2$ reaction. It is expected that both the ground (1^1A) and first excited (2^1A) PESs of the $O(^1D) + C_2H_6$ reaction are involved in the abstraction mechanism, while the possibility that it occurs via an intersystem crossing seems to be, in principle, less probable.

The experimental study of the $O(^1D) + C_2H_6$ reaction has been complemented by a theoretical analysis. To deal with this purpose, the same procedure (QCT method) and ab initio based analytical triatomic potential energy surfaces (PES1 and PES2) that were employed to analyze the related $O(^1D) + CH_4$ system have been applied here to study reaction 1. In this way, the dynamics of the insertion/fast elimination mechanism has been roughly described, qualitatively reproducing the experimental rovibrational distributions trends of the OH product reported in this work and in ref 8. This suggests that the additional complexity introduced by the presence of a C−C bond in ethane does not involve significant changes in the insertion/fast elimination microscopic mechanism of reaction 1 because it is quite a direct reaction mode. Moreover, the occurrence of a very small percentage (1−2%) of abstraction-like reactive trajectories in the QCT calculations on the $O(^1D) + C_2H_6$ ground PES has been observed, consistent with the experimental results.

Acknowledgment. This work was supported by the "Dirección General de Enseñanza Superior" of the Spanish Ministry of Education and Culture through the DGES Projects PB98-1209-C02-01 and PB98-1209-C02-02. J.H. thanks the CIRIT from the "Generalitat de Catalunya" (Autonomous Government of Catalonia) for a predoctoral research grant. The authors are also grateful to the "Generalitat de Catalunya" (Grants 1998SGR 00008 and 2000SGR 00016), to the "Centre de Supercomputació i Comunicacions de Catalunya (C^4-CESCA/CEPBA)" for computer time made available, and to Mr. Iván Antón for his help. This work is dedicated to the memory of our dear colleague Prof. Ernest Lluch.

References and Notes

(1) Wiesenfeld, J. R. *Acc. Chem. Res.* **1982**, *15*, 110.
(2) Warneck, P. *Chemistry of the Natural Atmosphere*; Academic: San Diego, CA, 1988.
(3) Burnett, E. B.; Burnett, C. R. *J. Atmos. Chem.* **1995**, *21*, 13.
(4) Matsumi, Y.; Tonokura, K.; Inagaki, Y.; Kawasaki, M. *J. Phys. Chem.* **1993**, *97*, 6816.
(5) Atkinson, R.; Baulch, D. L.; Cox, R. A.; Hampson, R. F., Jr.; Kerr, J. A.; Troe, J. *J. Phys. Chem. Ref. Data* **1985**, *14* (Suppl. 1).
(6) Atkinson, R.; Baulch, D. L.; Cox, R. A.; Hampson, R. F., Jr.; Kerr, J. A.; Rossi, M. J.; Troe, J. *J. Phys. Chem. Ref. Data* **1999**, *28*, 206.
(7) Shu, J.; Lin, J. J.; Lee, Y. T.; Yang, X. *J. Chem. Phys.* **2001**, *114*, 4.

(8) Park, C. R.; Wiesenfeld, J. R. *J. Chem. Phys.* **1991**, *95*, 8166.
(9) Luntz, A. C. *J. Chem. Phys.* **1980**, *73*, 1143.
(10) González, M.; Hernando, J.; Sayós, R.; Puyuelo, M. P.; Enríquez, P. A.; Guallar, J.; Baños, I. *Faraday Discuss.* **1997**, *108*, 453.
(11) Wada, S.; Obi, K. *J. Phys. Chem. A* **1998**, *102*, 3481.
(12) González, M.; Puyuelo, M. P.; Hernando, J.; Sayós, R.; Enríquez, P. A.; Guallar, J.; Baños, I. *J. Phys. Chem. A* **2000**, *104*, 521.
(13) Tsurumaki, H.; Fujimura, Y.; Kajimoto, O. *Chem. Phys. Lett.* **1999**, *301*, 145.
(14) Rudich, Y.; Hurwitz, Y.; Frost, J. G.; Vaida, V.; Naaman, R. *J. Chem. Phys.* **1993**, *99*, 4500.
(15) González, M.; Hernando, J.; Baños, I.; Sayós, R. *J. Chem. Phys.* **1999**, *111*, 8913.
(16) González, M.; Hernando, J.; Puyuelo, M. P.; Sayós, R. *J. Chem. Phys.* **2000**, *113*, 6748.
(17) Guallar, J.; Zorzano, M.; Zorzano, L. BOXDYE and LPDDYE (unpublished programs).
(18) Stark, G.; Brault, J. W.; Abrams, M. C. *J. Opt. Soc*. **1994**, *11*, 3.
(19) Luque, J.; Crosley, D. R. *LIFBASE: Database and Spectral Simulation Program*, version 1.5; Report 99-009; SRI International: Menlo Park, CA, 1999.
(20) Chidsey, I. L.; Crosley, D. R. *J. Quant. Spectrosc. Radiat. Transfer* **1980**, *27*, 187.
(21) Brozozowski, J.; Erman, P.; Lyyra, M. *Phys. Scr.* **1978**, *17*, 507.
(22) Bernstein, R. B.; Levine, R. D. *Advances in Atomic and Molecular Physics*; Bates D. R., Bederson, B., Eds.; Academic: New York, 1975.
(23) To calculate the prior distributions, we followed the same procedure previouly used in ref 8, although in the present work we performed an ab initio calculation in order to obtain the spectroscopic parameters of the C_2H_5 coproduct that are required to derive the energetically accessible states of this radical.
(24) González, M.; Puyuelo, M. P.; Hernando, J.; Martínez, R.; Sayós, R.; Enríquez, P. A. *Chem. Phys. Lett.*, in press.
(25) Honma, K. *J. Chem. Phys.* **1993**, *99*, 7677.
(26) Arai, H.; Kato, S.; Koda, S. *J. Phys. Chem.* **1994**, *98*, 12.
(27) González, M.; Hernando, J.; Millán, J.; Sayós, R. Work in progress.
(28) Hsu, Y.-T.; Wang, J.-H.; Liu, K. *J. Chem. Phys.* **1997**, *107*, 2351.
(29) Alagia, M.; Balucani, N.; Cartechini, L.; Casavecchia, P.; van Kleef, E. H.; Volpi, G. G.; Kuntz, P. J.; Sloan, J. J. *J. Chem. Phys.* **1998**, *108*, 6698.
(30) Hsu, Y.-T.; Liu, K.; Pederson, L. A.; Schatz, G. C. *J. Chem. Phys.* **1999**, *111*, 7931.
(31) Schatz, G. C.; Papaioannou, A.; Pederson, L. A.; Harding, L. B.; Hollebeek, T.; Ho, T. S.; Rabitz, H. *J. Chem. Phys.* **1997**, *107*, 2340.
(32) Drukker, K.; Schatz, G. C. *J. Chem. Phys.* **1999**, *111*, 2451.
(33) Gray, S. K.; Petrongolo, C.; Drukker, K.; Schatz, G. C. *J. Phys. Chem. A* **1999**, *103*, 9448.
(34) Aoiz, F. J.; Bañares, L.; Brouard, M.; Castillo, J. F.; Herrero, V. J. *J. Chem. Phys.* **2000**, *113*, 5339.
(35) Aoiz, F. J.; Bañares, L.; Castillo, J. F.; Brouard, M.; Denzer, W.; Vallance, C.; Hounvault, P.; Launay, J.-M.; Dobbyn, A. J.; Knowles, P. J. *Phys. Rev. Lett.* **2001**, *86*, 1729.
(36) Hoffmann, M. R.; Schatz, G. C. *J. Chem. Phys.* **2000**, *113*, 9456.
(37) Luntz, A. C.; Andresen, P. *J. Chem. Phys.* **1980**, *72*, 5842.
(38) Sweeney, G. M.; Watson, A.; McKendrick, K. G. *J. Chem. Phys.* **1997**, *106*, 9172.
(39) Luntz, A. C.; Andresen, P. *J. Chem. Phys.* **1980**, *72*, 5851.
(40) González, M.; Hernando, J.; Millán, J.; Sayós, R. *J. Chem. Phys.* **1999**, *110*, 7326.
(41) Mayne, H. R. *Int. Rev. Phys. Chem.* **1991**, *10*, 107.
(42) Sayós R.; González, M. TRIQCT (unpublished program).